Chemical Engineering Journal 155 (2009) 433–441

Contents lists available at ScienceDirect

Chemical Engineering Journal

journal homepage: www.elsevier.com/locate/cej

Intense UV-light absorption of ZnO nanoparticles prepared using a pulse combustion-spray pyrolysis method

I Made Joni [a], Agus Purwanto [a,b], Ferry Iskandar [a], Manabu Hazata [a], Kikuo Okuyama [a,*]

[a] Department of Chemical Engineering, Graduate School of Engineering, Hiroshima University, 1-4-1 Kagamiyama, Higashi Hiroshima, Hiroshima, 739-8527, Japan
[b] Department of Chemical Engineering, Faculty of Engineering, Sebelas Maret University, Jl. Ir. Sutami 36 A, Surakarta, Central Java, 57126, Indonesia

ARTICLE INFO

Article history:
Received 31 March 2009
Received in revised form 21 June 2009
Accepted 2 July 2009

Keywords:
ZnO
Pulse combustion
Optical property

ABSTRACT

We report the synthesis and characterization of ZnO nanoparticles prepared via pulse combustion-spray pyrolysis (PC-SP) at a high rate. Instead of using an ultrasonic nebulizer as the atomizer during PC-SP synthesis, a two-fluid nozzle was used to enhance the production rate. A high production rate was achieved by the use of a two-fluid nozzle, which efficiently generated droplets in large quantities, and by controlling the rate of precursor flow. ZnO nanoparticles were characterized using X-ray diffractometry (XRD), scanning electron microscopy (SEM), transmission electron microscopy (TEM) and UV–vis spectroscopy. The prepared ZnO nanoparticles were spherical and highly crystalline with an average size of 15.6 nm. In addition, high UV-light absorption and visible-light transparency properties were successfully obtained for a dispersion of ZnO nanoparticles in glycerol. The high UV-blocking capacity of the ZnO particle dispersion makes the dispersion potentially useful in cosmetic applications.

1. Introduction

Zinc oxide (ZnO) nanoparticles have attracted much interest because they possess various remarkable physical and chemical properties that are distinct from those of conventional bulk materials. ZnO is widely used for cosmetic applications because it is a chemically stable and environmentally friendly material that has good transparency and UV-blocking properties [1,2]. Many attempts have been made to synthesize ZnO nanoparticles that exhibit the desirable properties of ZnO. Continuous spray pyrolysis (SP) produces high-purity ZnO nanoparticles [3]. This type of SP method includes salt-assisted-SP (SASP) [4], low pressure-SP (LPSP) [5], and flame-SP (FSP) [6]. Our group recently introduced an SP method for the preparation of nanoparticles, which is called pulse combustion-SP (PC-SP) [7].

Evaporation from the pulse combustion (PC) engine occurs very rapidly because of acoustically high-fluctuating flow of the gas pressure and temperature during self-ignition [7,8]. The formation of ZnO particles using the PC-SP synthetic method depend on both the heat and pressure distribution and the characteristics of the atomizer. There are four characteristic parameters that are essential for the formation of ZnO particles: (1) heat distribution inside the furnace due to acoustically oscillating gas [9,10], (2) droplet precursor distribution behavior inside the furnace due to acoustically oscillating gas flow [11,12], (3) spray characteristics of precursor droplets [13], and (4) whether the addition of a heating furnace is necessary [7]. The PC-SP parameters of points (1) and (2) were estimated in both our previous studies [7], and in those of many other researchers, e.g., Zbicinski et al. [14], Kuts et al. [15], and Wang et al. [16]. The present study examines the effects of atomizer type, e.g., ultrasonic nebulizer or nozzle, on the spray characteristics of precursor droplets (point 3), and the addition of a heating furnace (point 4).

In our previous study, an ultrasonic nebulizer was used as the atomizer during PC-SP. However, this atomizer cannot be used for high production rate processing, which is a prerequisite for industrial application. Thus, the purpose of this study was to examine the use of a two-fluid atomizer for enhanced production of nanoparticles using PC-SP. In addition, the process parameters, such as precursor concentration, injection angle of the droplets and furnace temperature, were systematically investigated. Furthermore, the optical characteristics of a ZnO nanoparticle-glycerol dispersion were also evaluated. The UV-blocking of as-prepared ZnO is comparable to the counterpart of commercial ZnO nanoparticles, and the transparency of as-prepared ZnO is superior to commercial ZnO.

2. Experimental detail

The PC-SP experimental setup used to prepare ZnO nanoparticles is shown schematically in Fig. 1. The PC-SP setup consisted of a pulse combustor, a furnace, an electrostatic precipitator, a filtration system, and an atomizer (two-fluid nozzle). The ratio of

* Corresponding author. Tel.: +81 82 424 7716; fax: +81 82 424 5494.
E-mail address: okuyama@hiroshima-u.ac.jp (K. Okuyama).

1385-8947/$ – see front matter © 2009 Elsevier B.V. All rights reserved.
doi:10.1016/j.cej.2009.07.011

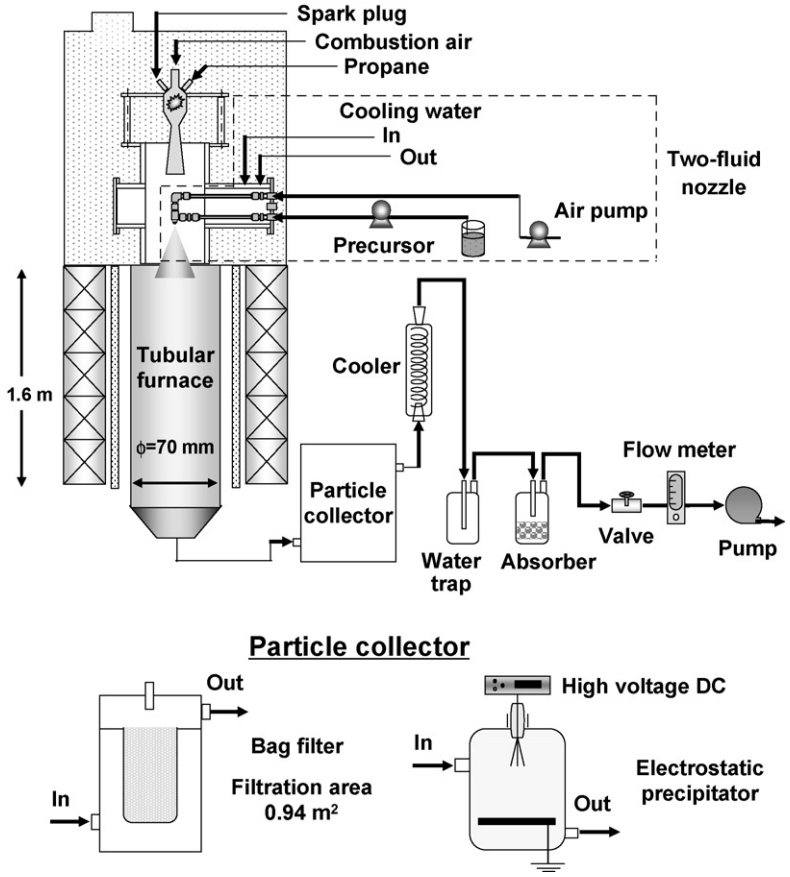

Fig. 1. Schematic of the PC-SP system with a two-fluid nozzle.

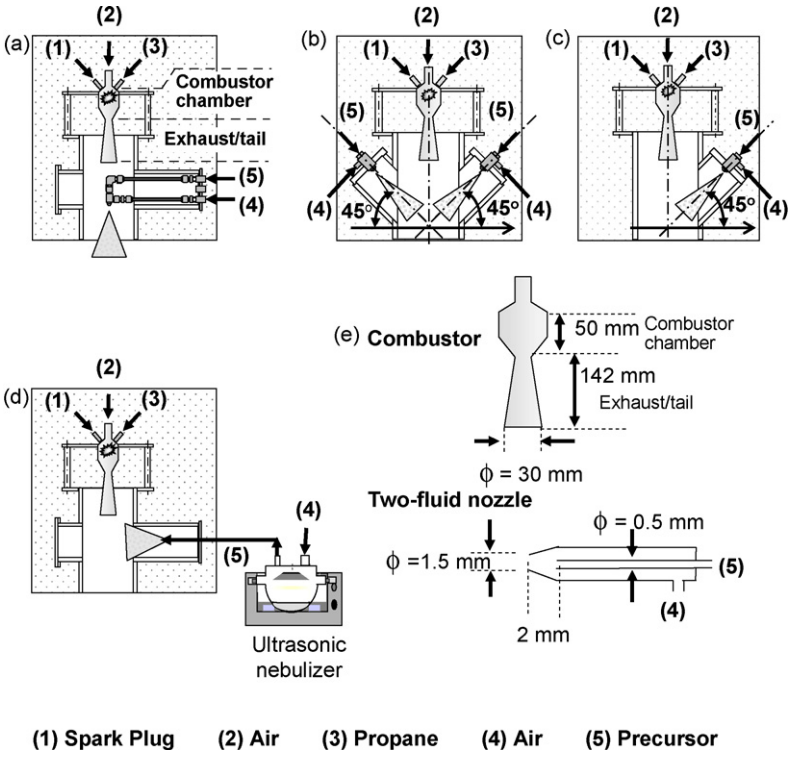

Fig. 2. Different configurations of the two-fluid nozzle—(a) condition I: inline with the direction of the oscillating gas stream, (b) condition II: double nozzle each at an injection angle of 45° relative to the direction of the oscillating gas stream, and (c) condition III: single nozzle position at an injection angle of 45° relative to the direction of the oscillating gas stream. The ultrasonic atomizer setup (d), and the dimension of combustor and two-fluid nozzle (e).

the flow rates (L/min) of the fuel (propane) to the oxidizer in the PC system (Pultech, Kobe, Japan) was fixed at 1:26.6. This ratio produced a pulse engine energy of 1000 kcal/h and 115 dB at a frequency of 1000 Hz. The detailed dimensions of the combustor are depicted in Fig. 2e. A flow meter controller (GCD-136X, Ulvac Kiko Inc., Kanagawa, Japan) was applied to maintain the particle flow rate at 90 L/min for provision of a constant residence time inside the furnace. An electrostatic precipitator was used for particle collection, except at high production rates, when a bag filter was used. The water trap and absorber of the filtration system were used to condense the water vapor in the outlet gas stream.

Alignment of the nozzle was investigated using three different configurations, as shown in Fig. 2. The first configuration (condition I, Fig. 2a) was a single nozzle positioned inline with the oscillating gas stream. The second configuration (condition II, Fig. 2b) was a double nozzle arrangement with one nozzle positioned at −45° and the other at 45° relative to the direction of the oscillating gas stream. The third configuration (condition III, Fig. 2c) was a single nozzle positioned at an angle of 45° relative to the gas stream. The dimensions of the two-fluid nozzle are depicted in Fig. 2e.

The precursor was prepared by dissolving zinc acetate dihydrate (99%, Wako Pure Chemical, Tokyo, Japan) in ultra-pure water. Different zinc acetate precursor concentrations were prepared, depending on the desired experimental conditions. The precursor air flow and feed rates were fixed at 10 and 250 mL/h, respectively, with the exception of the double-nozzle experiment (condition II, Fig. 2b) that used a precursor feed rate of 125 mL/h. The pipe carrying the precursor to the furnace inlet was water-cooled to prevent precipitation in the nozzle tip.

First, the combustor was set up with a propane to oxidizer ratio of 1:26.6. The prepared precursor was then fed to the tail of the combustor with the desired experimental configuration of two-fluid nozzle condition I, II, or II, and at different feed rates of 150, 250, or 500 mL/h. The produced particles were collected using either an electrostatic precipitator or a bag filter. Particles produced from various experimental setups then were subjected to various characterizations. Also, the performance of particles produced from condition I at a feed rate of 250 mL/h were compared to the performance of particles produced using the ultrasonic atomizer (NE-U17, Omron Healthcare Co. Ltd., Tokyo, Japan) operated at 1.7 MHz. Secondly, evaluation of the additional heating furnace was investigated at furnace temperatures of 300 °C (PC-SP300), 500 °C (PC-SP500) and 800 °C (PC-SP800). In this case, the two-fluid nozzle was set up with the configuration of condition I and a feed rate of 250 mL/h. The performances of PC-SP300, PC-SP500 and PC-SP800 were compared to a system that used only a pulsating combustor (PC).

A spray particle analyzer system (Spraytec, Malvern Instruments, Ltd., Malvern, UK) was used for the measurement of droplet size. This was a diode laser-based system with a wavelength of 670 nm and a beam diameter of 1.0×10^{-2} m. It was designed to continuously measure particle size distribution at measurement rates as high as 2.5 kHz. The crystallinity of the as-prepared ZnO nanoparticle powder was characterized by X-ray diffractometry (XRD, RINT 2200 V, Rigaku, Japan) using nickel-filtered Cu Kα radiation (λ = 1.54 Å) at 40 kV and 30 mA. The step and scanning rates of the XRD used in the measurement were 0.020° and 4°/min, respectively. A field-emission scanning electron microscope (FE-SEM, S-5000, Hitachi Ltd., Tokyo, Japan) operated at 20 kV was used to obtain images of the morphology of the produced ZnO particles. A field-emission transmission electronic microscope (FE-TEM, JEM-3000F, JEOL, Tokyo, Japan) operated at 300 kV was also used to analyze crystal structure and morphology. The optical properties of both the as-prepared ZnO particles and commercial ZnO (FINEX-50S-LP2, Sakai Chemical Industry Co. Ltd., Japan) were evaluated using UV–vis spectroscopy (U-2810, Hitachi, Japan). Prior to analysis, varying amounts of ZnO nanoparticles were dispersed in glycerol using a homogenizer at a rotation speed of 13,500 rpm for 30 min to produce dispersions of different concentrations. Particle size distribution before and after dispersion was measured using dynamic light scattering with an HPPS-5001 Malvern Instrument.

3. Results and discussion

To improve the rate of ZnO nanoparticle production using the PC-SP method, we used a two-fluid nozzle atomizer to deliver the precursor to the pulsating zone. Droplets generated using an ultrasonic nebulizer differ from those produced using two-fluid nozzle atomizers in droplet size, droplet capacity, and droplet flow pattern. A detailed investigation of the relationship between precursor properties and the droplets generated using an ultrasonic nebulizer atomizer was reported previously by our group [17]. The droplets generated using a two-fluid nozzle (approximately 20 μm) were larger than those produced using the ultrasonic nebulizer (approximately 6 μm), as shown in Fig. 3. However, a two-fluid nozzle can generate a large quantity of droplets by simply controlling the rate of precursor flow, regardless of the precursor properties (such as surface tension, concentration, temperature, etc.). A challenge associated with the use of a two-fluid nozzle atomizer is the generation of a chaotic flow pattern from a rapidly dispersing gas, which may affect the flow characteristics of the entire PC-SP system. Thus, in this study, we developed a strategy to produce nano-sized ZnO and high crystallinity of particles using a two-fluid nozzle atomizer. Furthermore, the optical properties of the ZnO nanoparticles-glycerol system were compared with those of commercial ZnO nanoparticles.

Fig. 4 shows both the SEM images and XRD pattern of ZnO particles prepared using either an ultrasonic atomizer or a two-fluid nozzle. Identical experimental conditions—1000 kcal/h of PC energy and 0.1 M precursor—were used for both setups. When the two-fluid nozzle was used, the precursor feed rate was 250 mL/h and the carrier air flow rate was 8.3 L/min. PC-SP with the two-fluid nozzle produced finer particles with greater crystalline size (Fig. 4a) compared with those produced using the ultrasonic atomizer (Fig. 4b). The atomizer of the ultrasonic nebulizer and two-fluid nozzle setups produced a different droplet size and flow pattern in the heating zone. The pressure difference between the liquid and solid nanoparticles inside the droplets, induced by rapid drying and evaporation rate, is considered to be the main reason for particle formation [7,17]. Thus, the different droplet sizes between the two methods coalesced with process parameters and derived different particle formations inside the furnace followed either by

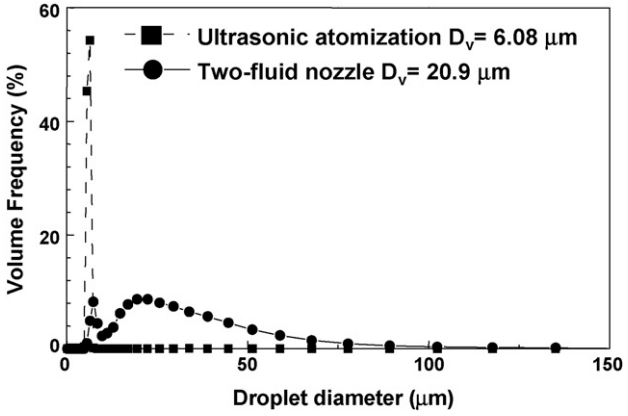

Fig. 3. Comparison of the droplet-size using either an ultrasonic atomizer or two-fluid nozzle with a precursor solution of 0.1 M, a precursor air carrier flow rate of 8.3 mL/min, and a precursor feed rate of 250 mL/h.

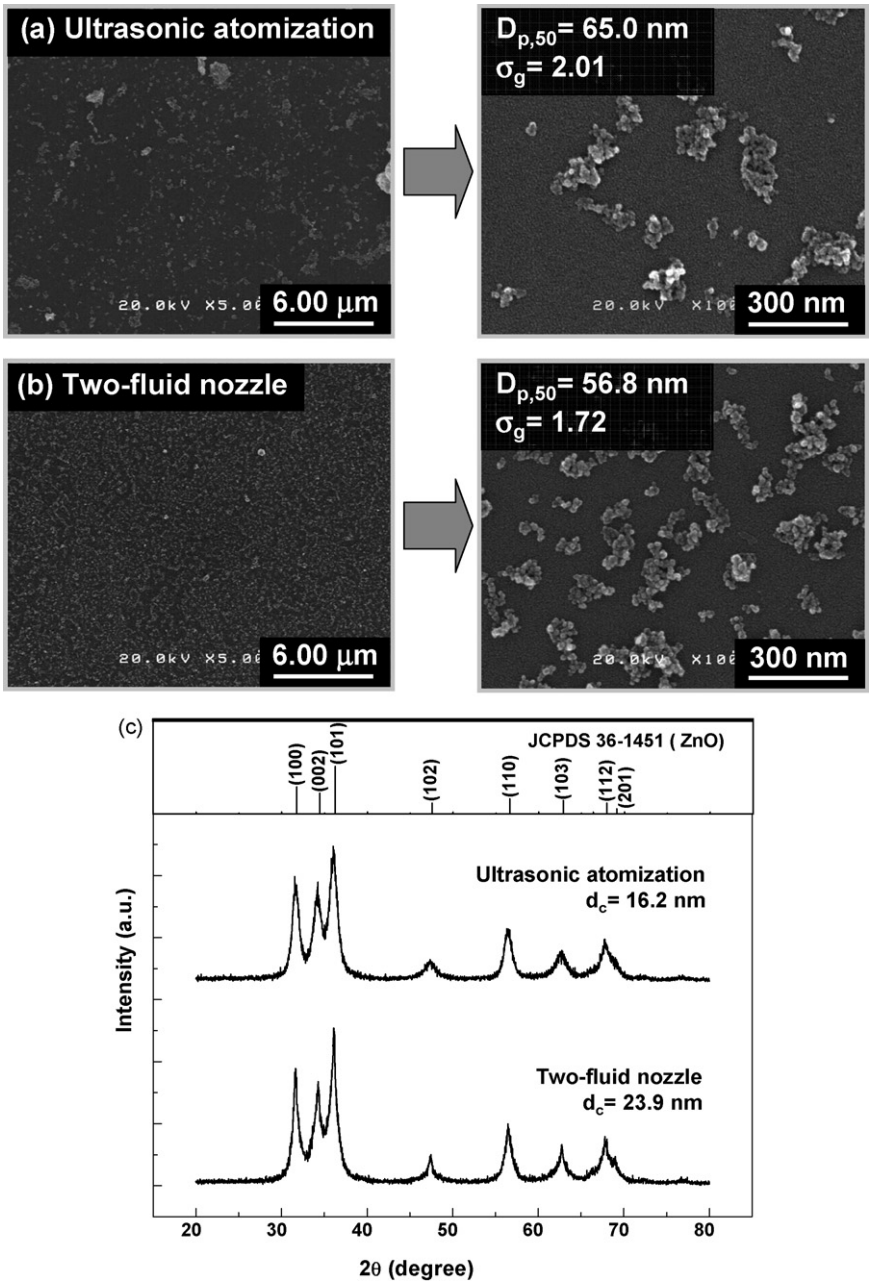

Fig. 4. FE-SEM images of particles produced using PC-SP with: (a) ultrasonic atomizer or (b) two-fluid nozzle, and XRD patterns of ZnO particles produced using ultrasonic atomizer compared with using two-fluid nozzle.

agglomeration or fragmentation. The ultrasonic nebulizer used as an atomizer (Fig. 2d) produced a low speed of the initial droplet and caused an increase in the resident time of the droplet inside the tubular furnace. In addition, droplets entered the lower region of the heat zone due to the technical difficulty of placing the nebulizer in the central heating zone. This setup derived lower crystalline growth, and the particles tended to agglomerate during the pyrolysis process in the tubular furnace. In contrast, the use of a two-fluid nozzle allowed the nozzle to be placed in the central heating zone. This condition caused the droplets to enter the higher region of the heat zone and rapidly evaporate to produce better crystal growth followed by fragmentation into finer particles. In addition, the speed of the initial droplet can be adjusted by controlling the precursor-feeding rate. The controllable initial speed of the droplet resulted in a controllable resident time, thus a smaller particle size could be obtained compared with that when using the ultrasonic atomizer (Fig. 4a and b).

In addition, use of the two-fluid nozzle with condition I at a feed rate of 250 mL/h successfully enhanced the rate of ZnO particle production to approximately 15 g/h using a bag filter as the particle collector. By contrast, under the same experimental conditions, the rate of ZnO nanoparticle production using the ultrasonic nebulizer was only 0.1 g/h. Because the production rate is also related to precursor concentration, a higher production rate might be achieved by increasing the precursor concentration. For this reason, the characteristics of the two-fluid nozzle in the PC-SP system were systematically investigated.

Fig. 5 shows the FE-SEM images and XRD patterns of ZnO nanoparticles prepared using the three different nozzle configurations (shown in Fig. 2a–c) and a precursor concentration of

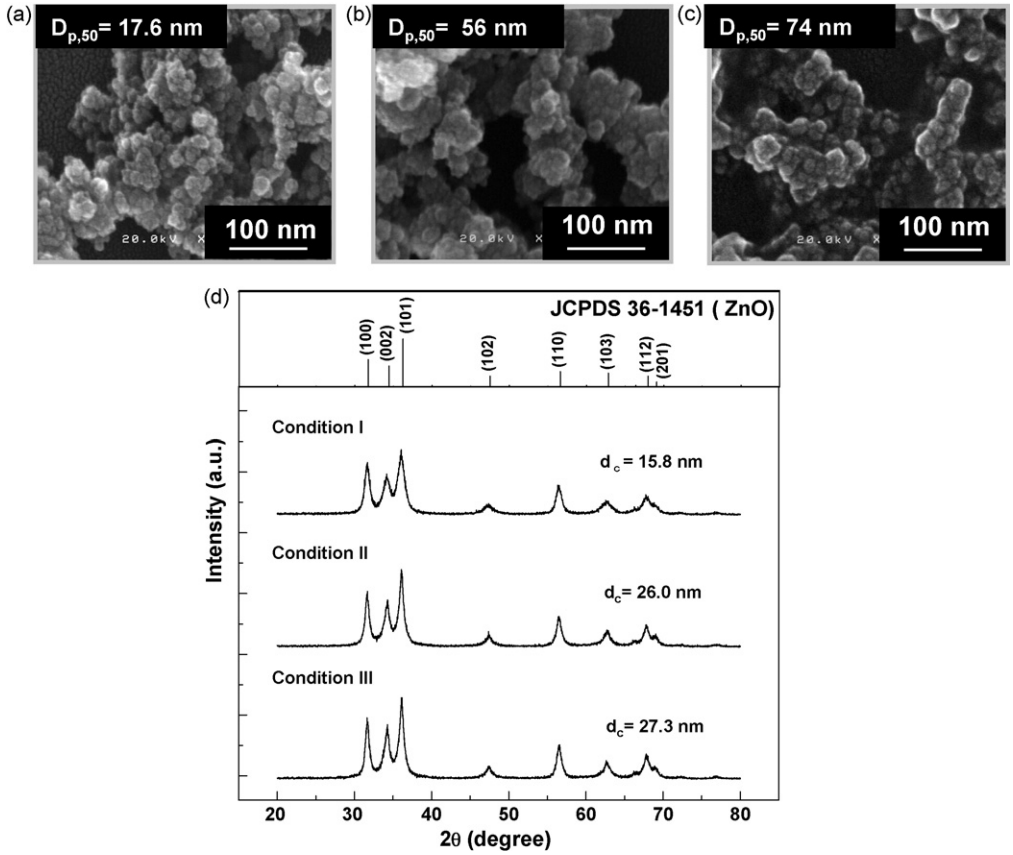

Fig. 5. FE-SEM images of ZnO particles produced using a spray nozzle: (a) condition I, (b) condition II, (c) condition III, and (d) XRD pattern of ZnO particles produced using condition I, II and III compared with reference JCPDS 36-1451.

0.6 M. The average sizes of SEM images were 17.6, 56 and 74 nm for conditions I, II and III, respectively (Fig. 5a–c). All configurations produced spherical ZnO nanoparticles. However, the degree of nanoparticle dispersion varied among configurations. Condition I (Fig. 2a) produced a smaller average size of nanoparticles with less agglomeration (Fig. 5a). In addition, the crystallite sizes of the ZnO nanoparticles were 15.8, 26.0, and 27.3 nm for the particles prepared using condition I, II, and III, respectively (Fig. 5d). Crystalline size was determined using the method of Scherrer by measurement of the full-width at half-maximum of the diffraction peak at [1 0 1] crystal orientation. The production of relatively un-agglomerated ZnO nanoparticles using condition I may result from the rapid evaporation of solvent from the droplets. When droplets were sprayed into the stream region, they oscillated in the phase and direction of the oscillating gas stream. Therefore, the velocities of both the gas and droplet may oscillate periodically at the same frequency [8,11,18,19]. A pressure difference between liquid and solid particles within the droplets induces rapid droplet evaporation, which causes fragmentation of primary particles [11,20]. Therefore, the configuration of condition I was used for further investigation due to a resultant smaller average size of particles.

Fig. 6a–c shows FE-SEM images of ZnO particles produced using precursor feed rates of 150, 250, and 500 mL/h, respectively, with the two-fluid nozzle in condition I, and a precursor concentration of 0.3 M. The average particle sizes of SEM images were 102, 96.4 and 72.3 nm corresponding to feed rates of 150, 250, and 500 mL/h. XRD patterns of ZnO particles produced using different precursor feed rates are compared with reference JCPDS 36-1451 in Fig. 6d. ZnO particles produced using a precursor feed rate of 150 mL/h showed increased crystalline (Fig. 6d) growth because the slower initial droplet speed resulted in longer droplet resident times relative to the other feed rates. However, partially agglomerated and larger ZnO particles were obtained (Fig. 6a). When a feed rate of 150 mL/h was subjected to further investigation, i.e. when the higher concentration was used it produced a higher average size of particles because the initial droplet size tended to increase with the increase in concentration. The opposite argument applied in the case of a feed rate of 500 mL/h. Therefore, the optimal precursor feed rate was determined to be 250 mL/h based on both average size and crystalline size of the produced particles. When further variation of other variables such as concentration and additional temperature and time in the heating furnace were used, it was reasonable to further investigate a precursor feed rate of 250 mL/h.

The effect of precursor concentration (C_{pre}) on the average particle size and crystallinity of the ZnO nanoparticles is shown in Fig. 7. The mean particle sizes of the SEM images of ZnO nanoparticles were 56.8, 96.4, 155 and 200 nm using precursor concentrations of 0.1, 0.3, 1 and 1.5 M, respectively. Thus, mean particle size tends to increase with precursor concentration, as shown in Fig. 7b. The crystallite size (d_c) of the as-prepared ZnO nanoparticles was 23.9, 22.8, 14.8 and 12.6 nm using precursor concentrations of 0.1, 0.3, 1 and 1.5 M, respectively. The opposite tendency was observed for the XRD characterization (Fig. 7a): crystalline size was decreased to the increase of precursor concentration. In general, both mean particle size and crystallite size were dependent on the precursor concentration, which is consistent with a previous report [7,17]. A plausible mechanism for the effect of precursor concentration on particle and crystallite size is as follows.

The PC-SP process can be summarized as follows: heat-up, evaporation of solution droplets, and formation of zinc oxide particles. The physical process before complete drying of droplets plays an important role in the fragmentation of precipitated particles.

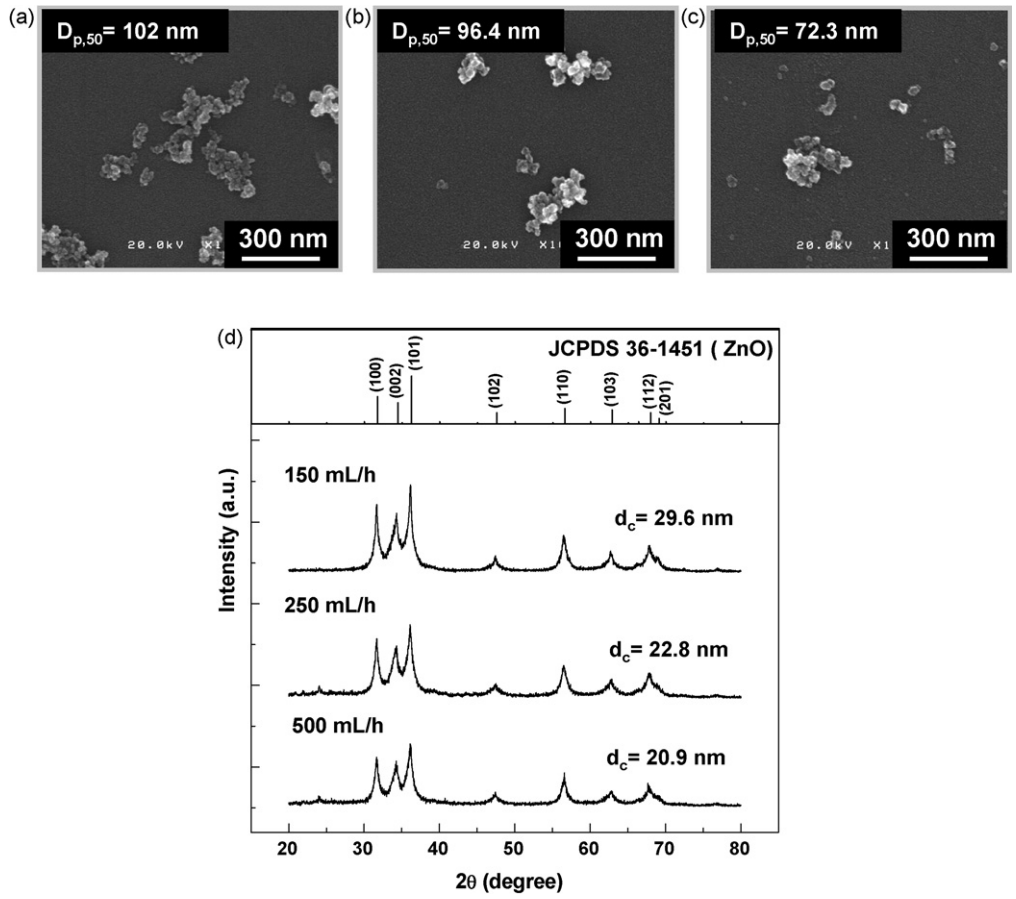

Fig. 6. FE-SEM images of ZnO particles produced using precursor feed rates of: (a) 150 mL/h, (b) 250 mL/h, (c) 500 mL/h, and (d) XRD pattern of ZnO particles produced using the different precursor feed rates compared with reference JCPDS 36-1451.

Soon after entering the pulsating zone, solvent evaporates from the droplets, which consist of the solute (zinc acetate dihydrate) and the solvent (water). Due to evaporation, saturation is achieved more rapidly with the use of high-concentration precursors. Consequently, precipitated particles accumulate within the droplets from the rapid nucleation process. If we focus on a single droplet, a micron-sized droplet acts as a spherical colloidal system (precipitated particles and water).

In a heated colloidal droplet, there are two types of pressure that interact: Laplace pressure and osmotic pressure. Laplace pressure is associated with the interfacial surface tension (γ), the surface area of the droplets (A), and is defined by the equation, $P = 2\gamma/R$, where R is the macroscopic radius of droplets. Meanwhile, the osmotic pressure generated from the interaction potential among colloids within the droplets can be evaluated using DLVO theory [20]. In PC-SP systems, the pulsating pressure generated from the combustion engine also contributes to fragmentation of the precipitated particles. If we assume that the pulsating pressure is identical in all experiments, analysis of the concentration effect is limited to only Laplace and osmotic pressures. As described above, a more highly concentrated precursor produces droplets with a higher concentration of precipitated particles. Consequently, Laplace pressure is increased, which generates precipitated particles within the droplets. By contrast, lower precursor concentrations lead to faster droplet fragmentation if osmotic pressure is greater than Laplace pressure. If rapid fragmentation occurs, growth of precipitated particles is diminished. As a result, the fragmented particles are smaller than those produced using high precursor concentrations. Thus, smaller nanoparticles result from lower precursor concentrations as indicated in Fig. 7b.

To improve the crystallinity of ZnO nanoparticles, additional heating with an electrical furnace was evaluated. The morphology and crystallinity of the as-prepared ZnO nanoparticles is shown in Fig. 8. The FE-SEM images of ZnO nanoparticles produced using either PC or PC-SP800 are shown by the arrows in the figure indicating the corresponding XRD pattern. Additional heating with an electrical furnace improved the crystallinity of the as-prepared ZnO nanoparticles. This result is consistent with other reports that heating nanoparticles enhances their crystallinity [7]. The mean particle sizes of the SEM images were 15.3 and 30.8 nm for the PC and the PC-SP800, respectively. The average size of the particles was increased with increased exposure to the heating furnace. In addition, nanoparticles produced from PC-SP800 were partially sintered. However, the nanoparticles remained spherical in morphology with no surface deformation, as shown in the FE-SEM images.

Fig. 9 shows the TEM images of both as-prepared and commercial ZnO nanoparticles. The as-prepared ZnO nanoparticles used a precursor concentration of 0.6 M with a single nozzle configuration and spray angle of 0° (without addition of heating furnace). Both the as-prepared and commercial ZnO nanoparticles were spherical and highly crystalline, as indicated by the ordered strong lattice fringes. ZnO nanoparticles produced using PC-SP had a smaller average diameter (15.6 nm) compared with the commercial particles (20.6 nm). The crystal lattice spacing of both the as-prepared ZnO and commercial ZnO particles was reconfirmed with their crystal lattice spacing from the XRD measurement. We found that crystal lattice spacing from HRTEM analysis was 2.7 and 2.5 Å for the crystal orientation of [1 0 0], respectively, for as-prepared and commercial ZnO. The lattice spacing of ZnO was 2.814 Å based on the JCPDS

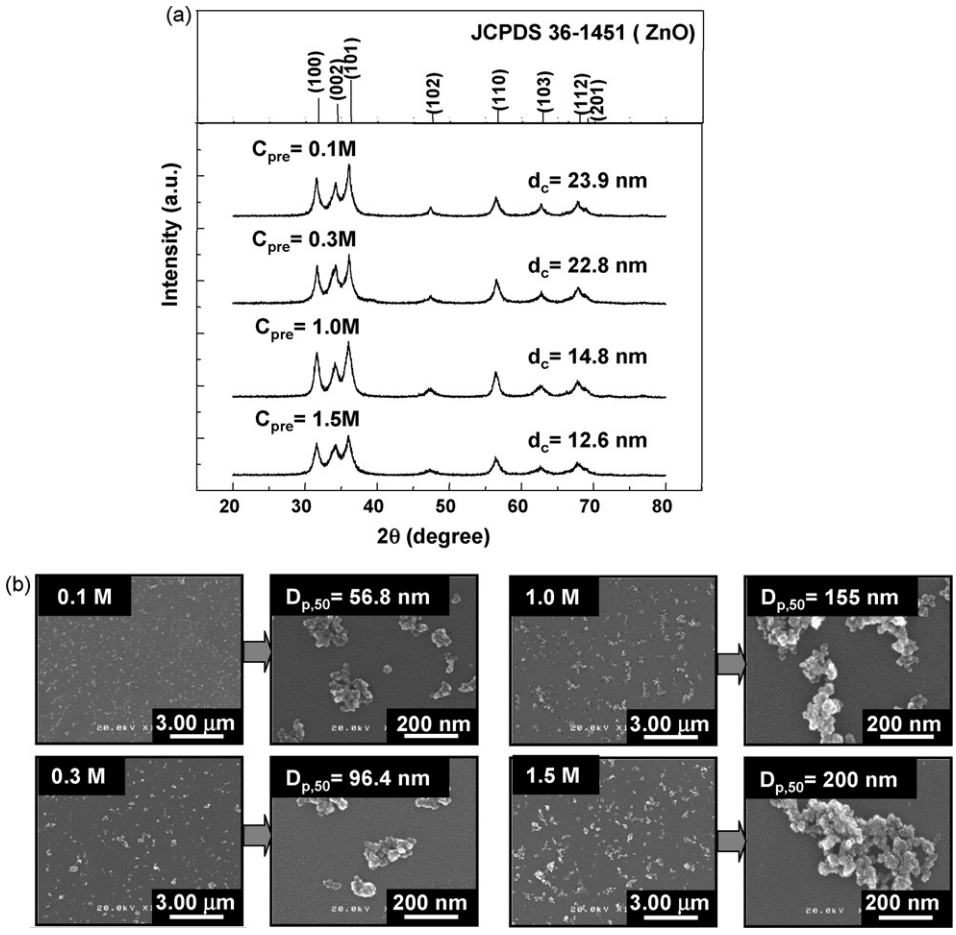

Fig. 7. (a) XRD pattern for particles produced using different precursor concentration compared with the reference JCPDS 36-1451 and (b) FE-SEM images of ZnO particle size prepared using different precursor concentrations.

36-1451 in the crystal orientation of [1 0 0]. The XRD measurement of as-prepared ZnO and commercial ZnO resulted in a crystal lattice spacing of 2.677 and 2.585 Å, respectively. This confirmed that the crystal of both as-prepared ZnO and commercial particles was shrinking in the direction of [1 0 0]. For evaluation of optical properties, different concentrations of ZnO nanoparticle dispersions in glycerol were prepared. Gycerol was chosen for solvent dispersion because of its use in cosmetic applications. The UV absorption and

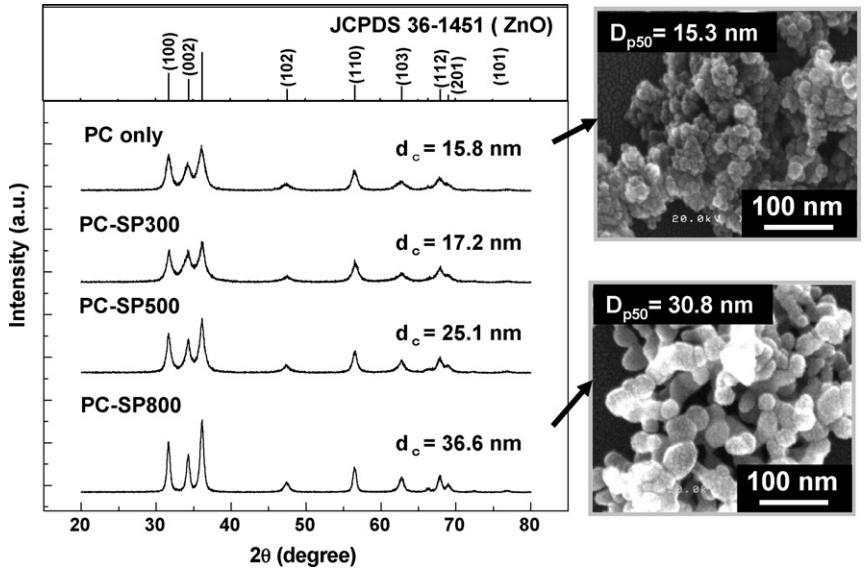

Fig. 8. XRD characteristics of ZnO particles produced using condition I with a precursor concentration of 0.6 M at different heating furnace temperatures: PC, 300 °C, 500 °C and 800 °C compared with the reference JCPDS 36-1451; and corresponding FE-SEM images of PC and PC-SP800.

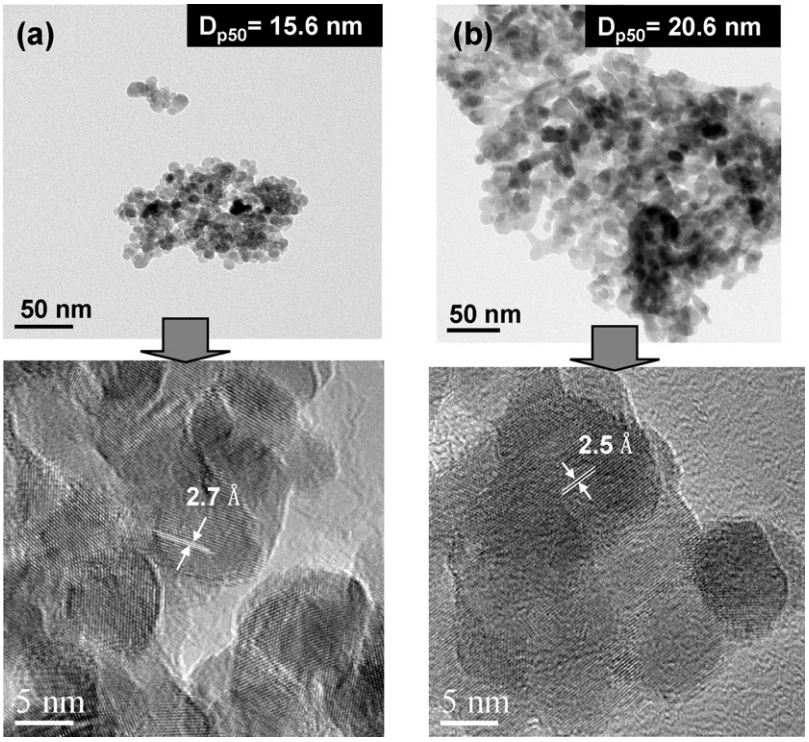

Fig. 9. High-resolution transmission electronic microscopic (HRTEM) images of ZnO particles: (a) particles produced using PC-SP with a 0.6 M zinc acetate dehydrate precursor solution, a single nozzle at a spray angle of 0°, and without addition of a heating furnace, (b) commercial particles.

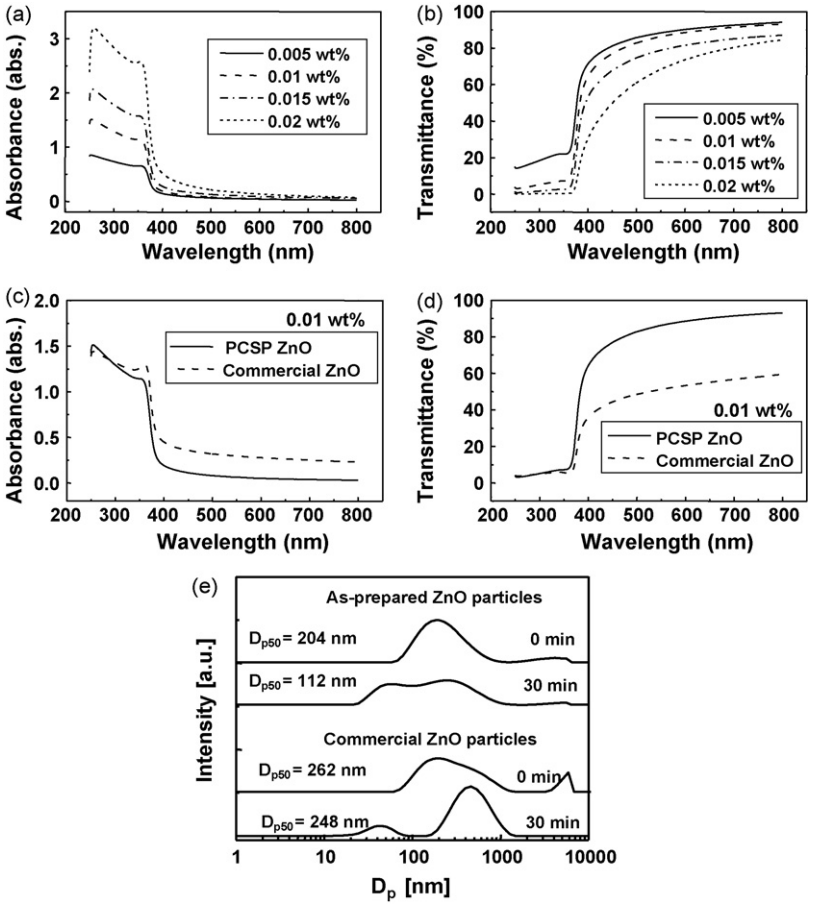

Fig. 10. Optical properties of ZnO nanoparticles with an average size of 15.8 nm dispersed in glycerol: (a) UV absorption and (b) transmittance. Comparison of the optical properties of as-prepared ZnO nanoparticles and commercial ZnO (Sakai Chemical Industry Co. Ltd., Japan) particles dispersed in glycerol both at 0.01 wt%: (c) UV absorption and (d) transmittance. (e) Size distribution of as-prepared and commercial ZnO particles dispersion in glycerol with 0.01 wt% ZnO in condition of before and after dispersion.

transmittance spectra of various concentrations (0.005–0.02 wt%) of the ZnO nanoparticle-glycerol dispersion are shown in Fig. 10a and b, respectively. The optical properties (absorbance and transmittance) of the ZnO–glycerol dispersions were highly dependent on the ZnO nanoparticle concentration. The correlation between optical properties and concentration in dispersion systems is well known. To evaluate the quality of ZnO nanoparticles prepared using a PC-SP system, the as-prepared particles were compared with commercial ZnO nanoparticles (Fig. 10c and d). The optical properties were measured at a dispersion concentration of 0.01 wt%. ZnO nanoparticles prepared using PC-SP had a UV absorption that was comparable to that of commercial nanoparticles. This is because PC-SP-prepared ZnO nanoparticles have a surface area that is comparable to that of commercial particles [21–23]. In addition, PC-SP ZnO nanoparticles exhibited better transparency (in the visible-light range) compared with that of commercial particles. The superior transparency of the ZnO nanoparticles prepared using PC-SP may be due to the enhanced dispersion of nanoparticles with less agglomeration. This was evidently supported by the size distribution comparison of the dispersion of as-prepared and commercial ZnO particles in glycerol as shown in Fig. 10e. Theoretically, agglomerated nanoparticles in the dispersion would cause multiple scattering of the incident visible-light, reducing the transparency of the dispersion. Finally, the PS-CP with the two-fluid atomizer can produce ZnO nanoparticles at a high rate. Moreover, the as-prepared ZnO nanoparticles exhibit high UV-blocking capacity, which makes the nanoparticles potentially useful in cosmetic applications. However, more investigation into ZnO nanoparticles is needed prior to acknowledging that ZnO nanoparticles are definitely safe for use in cosmetic application or in sunscreens.

4. Conclusions

The characteristics of the as-prepared ZnO nanoparticles could be controlled using PC-SP with a two-fluid nozzle. Continuous PC-SP with a two-fluid nozzle as the atomizer resulted in high purity of nano-sized ZnO particles at a high rate of production (15 g/h). Selection of the appropriate PC-SP system parameters resulted in spherical and highly crystalline nano-sized ZnO particles. A low-concentration dispersion of ZnO nanoparticles in glycerol exhibited excellent UV-light-shielding and transparency properties.

Acknowledgements

We acknowledge the Ministry of the National Education of the Republic of Indonesia for providing a doctoral scholarship (I.M.J). This study was financially supported by the Ministry of Education, Culture, Sports, Science and Technology (MEXT) Japan.

References

[1] A. Nasu, Y. Otsubo, Rheology and UV-protecting properties of complex suspensions of titanium dioxides and zinc oxides, J. Colloid Interface Sci. 310 (2007) 617–623.
[2] T. Iwasaki, M. Satoh, T. Masuda, T. Fujita, Powder design for UV-attenuating agent with high transparency for visible light, J. Mater. Sci. 35 (2000) 4025–4029.
[3] K. Okuyama, I.W. Lenggoro, Preparation of nanoparticles via spray route, Chem. Eng. Sci. 58 (2003) 537–547.
[4] C. Panatarani, I.W. Lenggoro, K. Okuyama, Synthesis of single crystalline ZnO nanoparticles by salt-assisted spray pyrolysis, J. Nanopart. Res. 5 (2003) 47–53.
[5] W.N. Wang, Y. Itoh, I.W. Lenggoro, K. Okuyama, Oxide nanoparticles prepared from nickel nitrate hexahydrate by a low pressure spray pyrolysis, Mater. Sci. Eng. B Solid 111 (2004) 69–76.
[6] A. Purwanto, I.W. Lenggoro, H.W. Chang, K. Okuyama, Preparation of submicron- and nanometer-sized particles of Y_2O_3:Eu^{3+} by flame spray pyrolysis using ultrasonic and two-fluid atomizers, J. Chem. Eng. Jpn. 39 (2006) 68–76.
[7] W. Widiyastuti, W.N. Wang, A. Purwanto, I.W. Lenggoro, K. Okuyama, A pulse combustion-spray pyrolysis process for the preparation of nano- and submicrometer-sized oxide particles, J. Am. Ceram. Soc. 90 (2007) 3779–3785.
[8] I. Zbicinski, A. Delag, C. Strumillo, J. Adamiec, Advanced experimental analysis of drying kinetics in spray drying, Chem. Eng. J. 86 (2002) 207–216.
[9] T. Schuller, D. Durox, S. Candel, Self-induced combustion oscillations of laminer premixed flames stabilized on annular burners, Combust. Flame 135 (2003) 525–537.
[10] A.V. Nguyen, H.J. Schulze, H. Stechemesser, G. Zobel, Contact time during impact of a spherical particle against a plane gas–liquid interface: theory, Int. J. Miner. Process. 50 (1997) 97–111.
[11] J.A. Carvalho, M.Q. McQuay, P.R. Gotac, The interaction of liquid reacting droplet with the pulsating flow in a rijke-tube combustor, Combust. Flame 108 (1997) 87–103.
[12] I.F. Murray, S.D. Heister, On a droplet's response to acoustic excitation, Int. J. Multiphase Flow 25 (1999) 531–550.
[13] W.N. Wang, I.W. Lenggoro, K. Okuyama, Dispersion and aggregation of nanoparticles derived from colloidal droplets under low-pressure conditions, J. Colloid Interface Sci. 288 (2005) 423–431.
[14] I. Zbicinski, C. Strumillo, M. Kwapinska, I. Smucerowicz, Calculations of the pulse combustion drying system, Energy Convers. Manage. 42 (2001) 1909–1918.
[15] P.S. Kuts, P.V. Akulich, N.N. Grinchik, C. Strumillo, I. Zbicinski, E.F. Nogotov, Modeling of gas dynamics in a pulse combustion chamber to predict initial drying process parameters, Chem. Eng. J. 86 (2002) 25–31.
[16] L. Wang, H. Sunada, F.D. Cui, Improvement of the dissolution rate of the insoluble drug—a pulse combustion dryer system, Pharm. Technol. Jpn. 22 (2006) 47–51.
[17] W.N. Wang, A. Purwanto, I.W. Lenggoro, K. Okuyama, H. Chang, H.D. Jang, Investigation on the correlation between droplet and particle size distribution in ultrasonic spray pyrolysis, Ind. Eng. Chem. Res. 47 (2008) 1650–1659.
[18] S.L. Fraenkel, L.A.H. Nogueira, J.A. Carvalho, F.S. Costa, Heat transfer coefficients for drying in pulsating flows, Int. Commun. Heat Mass 25 (1998) 471–480.
[19] P.V. Akulich, P.S. Kuts, E.F. Nogotov, Unsteady-state wave flows of a gas–solid suspension with gas-flow-rate oscillations and their effect on the heat and mass transfer, Theor. Found. Chem. Eng. 38 (2004) 455–461.
[20] S. Lyonnard, J.R. Bartlett, E. Sizgek, K.S. Finnie, T. Zemb, J.L. Woolfrey, Role of interparticle potential in controlling the morphology of spray-dried powders from aqueous nanoparticle sols, Langmuir 18 (2002) 10386–10397.
[21] M. Prutton, Introduction to Surface Physics, Oxford Science Publication, New York, 1994.
[22] B.K. Vainshtein, V.M. Frindkin, V.L. Indenbom, Structure of Crystals, third ed., Springer-Verlag, Berlin, 2000.
[23] S. Al-Hilli, M. Willander, Optical properties of zinc oxide nano-particles embedded in dielectric medium for UV region: numerical simulation, J. Nanopart. Res. 8 (2006) 79–97.